



## City Research Online

### City, University of London Institutional Repository

---

**Citation:** Phillips, J. P., Langford, R. M., Chang, S. H., Maney, K., Kyriacou, P. A. and Jones, D. P. (2010). Cerebral Arterial Oxygen Saturation Measurements Using a Fiber-Optic Pulse Oximeter. *Neurocritical Care*, 13(2), pp. 278-285. doi: 10.1007/s12028-010-9349-y

This is the accepted version of the paper.

This version of the publication may differ from the final published version.

---

**Permanent repository link:** <https://openaccess.city.ac.uk/id/eprint/13295/>

**Link to published version:** <http://dx.doi.org/10.1007/s12028-010-9349-y>

**Copyright:** City Research Online aims to make research outputs of City, University of London available to a wider audience. Copyright and Moral Rights remain with the author(s) and/or copyright holders. URLs from City Research Online may be freely distributed and linked to.

**Reuse:** Copies of full items can be used for personal research or study, educational, or not-for-profit purposes without prior permission or charge. Provided that the authors, title and full bibliographic details are credited, a hyperlink and/or URL is given for the original metadata page and the content is not changed in any way.

# Cerebral Arterial Oxygen Saturation Measurements Using a Fiber-Optic Pulse Oximeter

J. P. Phillips · R. M. Langford · S. H. Chang ·  
K. Maney · P. A. Kyriacou · D. P. Jones

## Abstract

**Background** A pilot investigation was undertaken to assess the performance of a novel fiber-optic cerebral pulse oximetry system. A fiber-optic probe designed to pass through the lumen of a cranial bolt of the type used to make intracranial pressure measurements was used to obtain optical reflectance signals directly from brain tissue.

**Methods** Short-duration measurements were made in six patients undergoing neurosurgery. These were followed by a longer duration measurement in a patient recovering from an intracerebral hematoma. Estimations of cerebral arterial oxygen saturation derived from a frequency domain-based algorithm are compared with simultaneous pulse oximetry ( $\text{SpO}_2$ ) and hemoximeter ( $\text{SaO}_2$ ) blood samples.

**Results** The short-duration measurements showed that reliable photoplethysmographic signals could be obtained from the brain tissue. In the long-duration study, the mean ( $\pm$ SD) difference between cerebral oxygen saturation ( $\text{ScaO}_2$ ) and finger  $\text{SpO}_2$  (in saturation units) was  $-7.47(\pm 3.4)\%$ . The mean ( $\pm$ SD) difference between  $\text{ScaO}_2$  and blood  $\text{SaO}_2$  was  $-7.37(\pm 2.8)\%$ .

**Conclusions** This pilot study demonstrated that arterial oxygen saturation may be estimated from brain tissue via a fiber-optic pulse oximeter used in conjunction with a

cranial bolt. Further studies are needed to confirm the clinical utility of the technique.

**Keywords** Pulse oximetry · Saturation · Cerebral · Fiber-optic · Cranial bolt

## Introduction

Patients recovering from head injury, stroke, or neurosurgery are particularly susceptible to further complications resulting from ischemia, in many cases leading to temporary or permanent disability and not uncommonly, in death [1–3]. Such ‘secondary’ injuries may be minimized by rapid administration of emergency treatment [4] and by careful management of the head injury in the hours or days following the injury [5]. Effective treatment depends on adequate and appropriate monitoring of the patient’s condition, including measurement or estimation of the availability of oxygen to the brain tissue. Such measurements are frequently performed using three common modalities; tissue oxygen partial pressure measurement [6], jugular venous bulb oximetry [7], and near-infrared spectroscopy [8].

Near-infrared spectroscopy (NIRS) is a noninvasive optical technique that can be used for monitoring brain tissue oxygen saturation, changes in blood volume and, indirectly, brain blood flow and oxygen consumption [9]. Computer models have shown, however, that the volume of tissue interrogated by NIRS typically consists of 30% brain and 70% noncerebral tissues (i.e., scalp and skull) [10]. Absorption of light by these tissues, particularly the blood within the scalp vasculature complicates algorithms used in NIRS systems and can lead to inaccuracies in these systems’ calculation of oxygen saturation [11, 12].

After introduction of  $PbtO_2$  catheters there is a minimum 'settling-in' time, during which measurements are unstable. This is typically approximately 2 h, but is sometimes much longer, probably due to micro-hemorrhages or possibly due to local vasoconstriction. In an animal study, small micro-hemorrhages were observed around the catheter tip that could cause falsely low  $PbtO_2$  readings [13]. An in vitro study showed  $PO_2$  values of  $0.93 \pm 0.19$  kPa in zero oxygen solution, suggesting that  $PbtO_2$  values may be overestimated when they are at critically low levels [6].

A fiber-optic based system for directly monitoring brain tissue hemoglobin oxygen saturation using photoplethysmography (PPG) has been developed [14]. The fiber-optic probe is placed in direct contact with the brain tissue via a cranial bolt (Integra Neurosciences, Plainsboro, NJ, USA) of the type used for the measurement of intracranial pressure (ICP) [15, 16], thereby eliminating tissue such as the scalp, skull, and dura from the optical path. The eventual aim is to produce a rapidly responding indicator of cerebral hypoxemia, which may be used for patients in whom the use of a cranial bolt is indicated for measurement of ICP.

This paper presents results from a pilot clinical trial of the developed fiber-optic system. Short-duration measurements were conducted in six patients undergoing neurosurgery at the Royal London Hospital, London, UK. The primary aim was to determine whether satisfactory PPG signals could be obtained from the brain tissue [17]. The study also aimed to verify whether the cranial bolt access system would serve as a suitable conduit for the fibers and whether the acquired signals would be adequate for calculation of oxygen saturation. Measurements of longer duration were also taken from a patient recovering from an intracerebral hemorrhage in the London Hospital Intensive Therapy Unit (ITU).

## Materials and Methods

### Measurement System

The measurement system for this study [18] has been developed and evaluated in our laboratory and is based around a fiber-optic reflectance PPG probe comprising two optical fibers, one of which is used to transmit light to the tissue and the other to return a fraction of the backscattered light to a photodetector. A signal processing system consisting of a circuit interfaced with a notebook computer has been implemented for calculation of clinical variables from the measured light intensities and is described below. Figure 1 shows a photograph of the measurement system showing the fiber-optic probe.

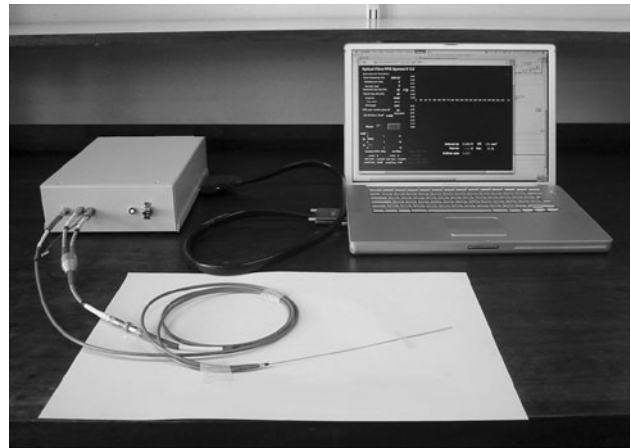


**Fig. 1** Photograph of the pulse oximetry measurement system showing the fiber-optic probe

The fiber-optic probe consists of two silica optical fibers (a transmitting fiber and a receiving fiber) each with a core diameter of  $400 \mu\text{m}$ , an outer cladding diameter of  $730 \mu\text{m}$  and a numerical aperture (NA) of 0.39 (Ocean Optics Inc., Dunedin, FL, USA). The distal end of each fiber is cut and polished flat and the proximal end terminated with a male SMA connector. The fibers are coated in a protective PVC jacket, which is stripped away over a length of 16 cm from the distal end. The probe materials are biomedically compatible, and allow steam sterilization at  $136^\circ\text{C}$ .

The light sources used are red and infrared light emitting diodes (LEDs) mounted in SMA packages (The Optoelectronic Manufacturing Corporation Ltd, Redruth, UK). The infrared LED used for the short-duration measurements has a peak emission wavelength of 850 nm, while the device used for the long-duration measurement has a peak emission at 940 nm. The red LED used for both studies has a peak emission wavelength of 660 nm. Both LEDs are connected to the single transmitting optical fiber using a Y-coupler, i.e., a bifurcated optical fiber assembly (Ocean Optics Inc., Dunedin, FL, USA). The photodetector is an SMA-packaged PIN photodiode of active surface area  $0.8 \text{ mm}^2$  (The Optoelectronic Manufacturing Corporation Ltd). The photodetector is coupled directly to the receiving optical fiber.

An instrumentation unit is used for the control of the light sources and acquisition of signals from the tissue. This hardware is interfaced to a 16-bit DAQCard-AI-16XE-50 data acquisition card (National Instruments Inc. Austin, TX, USA) installed into a notebook computer. The LEDs are driven by a pair of switchable regulated current sources, one for each wavelength, supplying 25 and 14 mA to the red and infrared LEDs, respectively. Timing signals are provided by a programmable counter timer built into the data acquisition card.

The photodiode is connected to a differential transimpedance amplifier. The output of the transimpedance amplifier is fed into a demultiplexer and the signals separated into three components, representing the infrared (IR), red (R), and ambient (AMB) light intensities. The total intensities of the red and infrared signals are obtained by filtering to remove high frequency switching noise from the demultiplexer using 2nd-order low-pass Butterworth filters each with a cut-off frequency of 16 Hz (at  $-3$  dB). The instrumentation is powered by two 12 V 1.2 Ah sealed lead-acid batteries (Yuasa Battery Inc., Laureldale, PA, USA).

The signals are all fed into the analog-to-digital converter built into the data acquisition card installed in the notebook computer running a LabVIEW (National Instruments Inc. Austin, TX, USA) Virtual Instrument (VI). The VI reads the digitized signals at a rate of 100 samples per second and records the signals in a spreadsheet file.

### Cranial Access System

The Integra Neurosciences IM-3 Cranial Access System was used in conjunction with the fiber-optic probe, allowing the tips of the optical fibers to be placed directly within the tissue of the cerebral cortex. The IM-3 system is designed to accommodate three sensors: an ICP sensor, a LiCox tissue oxygen partial pressure ( $PbtO_2$ ) sensor, and a temperature probe.

The triple-channel IM-3 bolt was used both for the preliminary evaluation of the fiber-optic cerebral pulse oximeter in neurosurgical patients and in the later study in ITU patients. The only neurophysiological monitoring currently used routinely in patients at the Royal London Hospital is ICP, so the use of a triple-channel bolt in these patients provides two unused lumens. The LiCox and temperature lumens were used to accommodate the optical fibers, leaving the third (larger) lumen free for ICP monitoring. The distance between the fibers once positioned in the bolt, measured from center to center, is 2.0 mm.

The IM-3 system is supplied in a sterile package containing a threaded cranial bolt, triple-lumen insert and insertion tools. Cranial bolts are routinely inserted under sterile conditions in head-injured patients. The insertion site depends upon the nature of the injury, but is usually in the temporal or parietal regions of the skull, and usually on the same side as the injury. The head is positioned with the insertion site uppermost and the head supported using sandbags or a 'horseshoe', a specialist surgical head-rest. The scalp is shaved and thoroughly disinfected and an approximately 3 cm incision made down to the bone. The pericranial tissue is stripped away and the skin is held back by self-retaining retractors. A burr hole is then carefully made in the skull using a twist drill, then the underlying

dura is punctured using a sharp perforator. The cranial bolt is screwed into the burr hole until the thread is almost concealed by the skull. The triple-lumen insert is passed through the lumen of the bolt so the distal end penetrates the brain tissue as shown in Fig. 2. A compression cap, which is attached to the body of the insert, is tightened onto a thread on the rear of the cranial bolt, compressing a hollow cylindrical silicone washer in the assembly, which expands, achieving a tight seal between the assembly and the bolt.

The luer hubs at the proximal end of the triple-lumen assembly are terminated with special luer-locking caps. Each cap has a patent channel through which the corresponding probe may be threaded. Tightening the cap causes longitudinal compression of a silicone washer, which expands inwards producing a seal around the probe. The intra-cranial bolt is designed to be left in place for several days enabling ICP and other measurements to be made while the patient remains in a critical condition. The self-sealing washers prevent contamination entering the burr hole, minimizing the risk of infection.

### Short-Duration Measurements

This study was approved by the local Research Ethics Committee and patients' written informed consent was

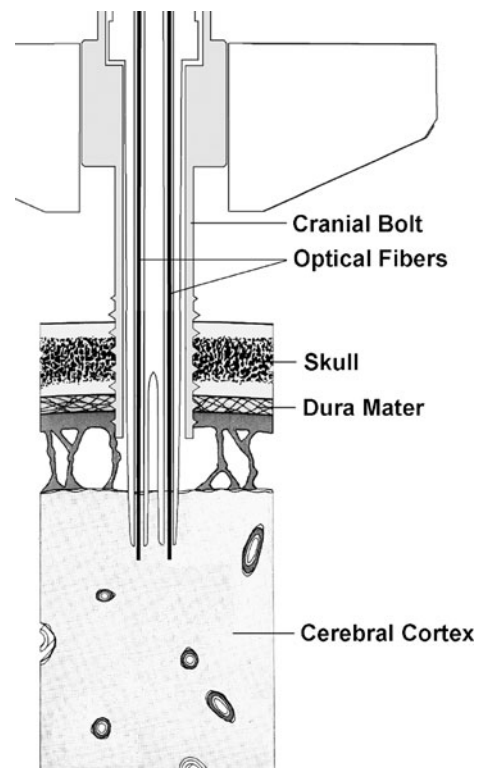


**Fig. 2** Cranial bolt and fibers in situ. The inter-fiber separation was 2.0 mm

sought prior to the study. The neurosurgical patients received a bolt temporarily prior to craniotomy for aneurism clipping ( $n = 2$ ) or excision/debulking of tumors ( $n = 4$ ). After induction of anesthesia, the patient was intubated and ventilated and the cranial bolt was inserted by the neurosurgeon. The fibers were then inserted via the bolt, approximately 5 mm into the brain and the luer caps tightened to form a seal around the fiber. Signals were recorded for several minutes at the discretion of the surgeons and theatre staff. Five millimeters was chosen as a suitable depth of penetration to ensure that the detected light was entirely from brain tissue and not from the dura and other surrounding tissue, and to ensure that the fibers protruded fully from the end of the cranial bolt assembly. The patient's arterial oxygen saturation was monitored using a commercial finger pulse oximeter. After the monitoring period, the fibers and the bolt were removed and the surgery resumed. To date, six male and female patients of mean ( $\pm$ SD) age 45.5 ( $\pm$ 19) years requiring elective neurosurgery have been studied.

#### Long-Duration Measurement

A 78-year-old female who presented to hospital with a Glasgow Coma Score (GCS) of 3 was studied for a longer period. A Computed Tomography (CT) scan revealed the presence of a frontal temporal intracerebral hematoma. The patient underwent a craniotomy to evacuate the hematoma. The patient was sedated with Propofol and stabilized according to established treatment protocols. A cranial bolt was placed into the right frontal part of the skull by a neurosurgical registrar and ICP monitoring, together with routine ITU monitoring commenced. After obtaining assent from the patient's relatives the optical fiber probe was introduced into the cranial bolt, so that the probe was penetrating the right frontal lobe of the cerebral cortex. Signals were recorded from the brain tissue using the cerebral pulse oximeter for a period of 6 h while the patient was in the ITU. A commercial pulse oximeter on the patient's finger recorded the arterial oxygen saturation. Blood samples were taken hourly from an indwelling arterial catheter for measurement of blood gases and oxygen saturation using a hemoximeter. The patient remained lightly sedated throughout the 6-h monitoring period and was mechanically ventilated throughout the monitoring period. After approximately 6 h the patient was moving frequently, and appeared to be regaining consciousness so the optical fibers were removed from the bolt and monitoring stopped. The patient remained in the ITU for several days where she made a satisfactory recovery.

#### Estimation of Oxygen Saturation Values

The short-duration red and infrared signals were analyzed retrospectively using 60-s samples of each waveform. This sample was chosen by visual inspection, selecting the 'best' signal in terms of overall quality of the waveform, where waveforms with large amplitude and minimal artifact were preferred. The arterial oxygen saturations were estimated from the cardiac-modulated components of the discrete Fourier transforms using a LabVIEW virtual instrument incorporating a fast Fourier transform algorithm.

The cardiac frequency  $f_{\text{card}}$  was derived from the discrete Fourier transform of the acquired signal. The amplitude of the pulse peaks in each amplitude spectrum were then calculated and normalized by dividing by the amplitude at zero frequency (i.e., the DC component) in each spectrum. The cerebral arterial oxygen saturation,  $\text{ScaO}_2$  was estimated using an empirically derived formula for estimating oxygen saturation in pulse oximetry from the 'ratio-of-ratios' (enclosed within the parentheses in the equation) [19]:

$$\text{ScaO}_2 = 110 - 25 \left( \frac{A_{\text{card,R}}/A_{\text{DC,R}}}{A_{\text{card,IR}}/A_{\text{DC,IR}}} \right) \quad (1)$$

where  $A_{\text{card,R}}$  and  $A_{\text{card,IR}}$  are the red and infrared cardiac peak amplitudes and  $A_{\text{DC,IR}}$  and  $A_{\text{DC,R}}$  are the amplitudes of the infrared and red spectra at zero frequency. The long-duration data was broken down into blocks of 60 s. A continual estimation of the arterial and venous oxygen saturations was thus produced from successive data blocks utilizing the same software algorithm used for the short-duration measurements.

The arterial oxygen saturation ( $\text{SpO}_2$ ) was manually recorded from the commercial finger pulse oximeter (GE Healthcare Clinical Systems, Wauwatosa, WI, USA) incorporated into the patient monitor and the arterial oxygen saturation ( $\text{SaO}_2$ ) was measured from a blood sample using a hemoximeter (IL682 CO-oximeter, Instrumentation Laboratory Inc., Lexington, MA, USA). A total of 54 pulse oximetry measurements and five hemoximeter measurements were recorded during the 6-h period.

## Results

#### Short-Duration Measurements

Signals were successfully obtained at both wavelengths for all six patients. To allow comparison of waveforms between patients, each waveform was normalized by dividing by the total intensity (i.e., the AC signal was

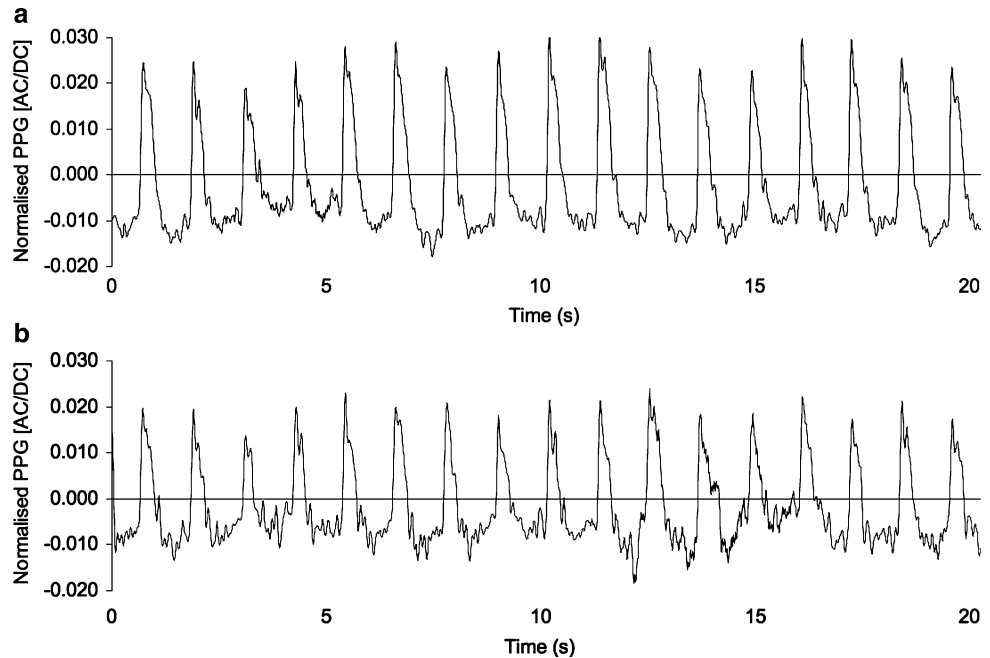
divided by the AC + DC signal). Figure 3 shows example waveforms. The infrared and red PPG signals are of good quality and the dicrotic notch is visible on both channels.

Figure 4 shows another waveform, obtained from a different patient. The PPG signals are dominated by a large low frequency modulation appearing on both the infrared and red channels. The frequency of the modulation

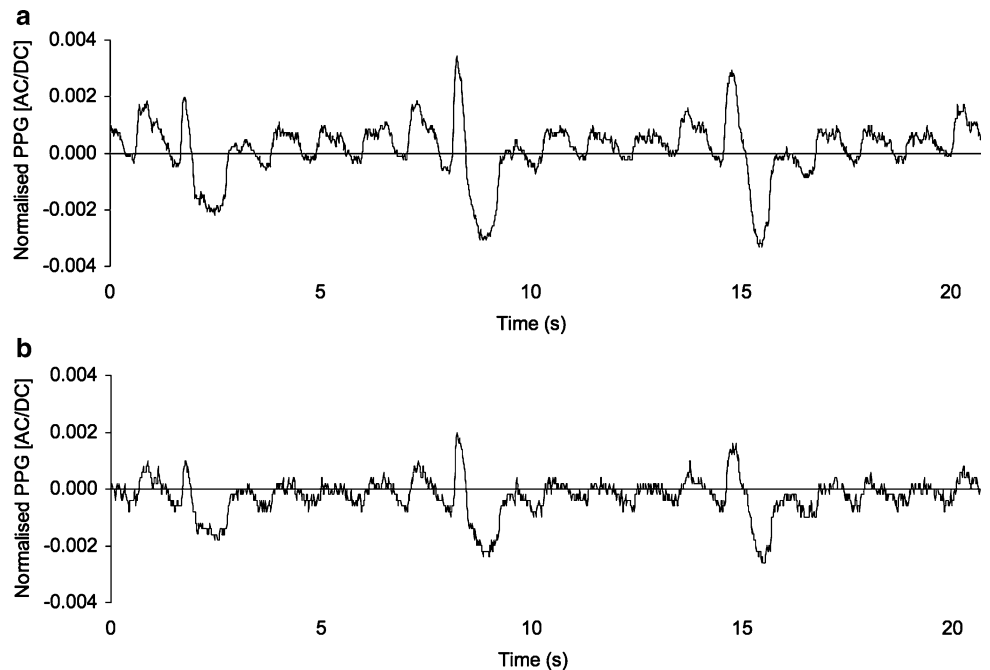
coincides with the ventilation frequency so this signal is thought to be caused by ventilator induced pressure changes in the cerebral circulation.

The acquired AC + DC signals for all the neurosurgical patients were used to estimate the cerebral arterial oxygen saturation  $ScaO_2$ , using an FFT algorithm. The results are summarized in Table 1.

**Fig. 3** Infrared (a) and red (b) normalized PPG signals recorded from Patient No. 6



**Fig. 4** Infrared (a) and red (b) normalized PPG signals recorded from Patient No. 3





## Long-Duration Measurement

Signals were successfully recorded from the patient throughout the 6-h monitoring period. Table 2 shows the cardiac frequency, normalized infrared and red peak amplitudes, ratio-of-ratios and ScaO<sub>2</sub> calculated from the Fourier transforms obtained from the acquired data. The main peak occurring in each 1-min red and infrared spectrum between 0.8 and 1.6 Hz (i.e., in the cardiac frequency range) was identified by the Virtual Instrument and the frequency and amplitude values averaged for the entire measurement period.

Figure 5 shows a graph of ScaO<sub>2</sub> (brain), SpO<sub>2</sub> (finger), and SaO<sub>2</sub> (blood sample) plotted against time for the entire measurement period. It can be seen from the graph that the ScaO<sub>2</sub> was generally significantly lower than the finger SpO<sub>2</sub> ( $P < 0.001$ ) and the blood SaO<sub>2</sub> ( $P < 0.001$ ) as confirmed by paired Student's *t*-tests. A steady trend of decreasing ScaO<sub>2</sub> was seen for the first 4 h followed by a gradual rise. The mean ( $\pm$ SD) difference between ScaO<sub>2</sub> and finger SpO<sub>2</sub> (in saturation units) was  $-7.47(\pm 3.4)\%$ ;  $n = 54$ . The mean ( $\pm$ SD) difference between ScaO<sub>2</sub> and blood SaO<sub>2</sub> was  $-7.37(\pm 2.8)\%$ ;  $n = 5$ .

Figure 5 also shows a graph of ICP against time, while Fig. 6 shows a graph of other variables recorded from the patient monitoring in the ITU plotted against time for the entire measurement period. The variables are: mean arterial pressure (MAP), cerebral perfusion pressure (CPP = MAP - ICP), and end-tidal carbon dioxide concentration (EtCO<sub>2</sub>). ICP values were within the normal range

**Table 1** Total measurement duration ( $T_1$ ) and duration of noise-free signal acquisition ( $T_2$ ) from short-duration signals

| Patient No. | $T_1$ (s) | $T_2$ (s) | Pulse frequency $f_{card}$ (Hz) | Ratio-of-ratios | ScaO <sub>2</sub> (%) |
|-------------|-----------|-----------|---------------------------------|-----------------|-----------------------|
| 1           | 260       | 162       | 1.06                            | 0.474           | 98.2                  |
| 2           | 276       | 167       | 1.08                            | 0.380           | 100.5                 |
| 3           | 339       | 286       | 0.94                            | 0.608           | 94.8                  |
| 4           | 148       | 76        | 0.94                            | 0.784           | 90.4                  |
| 5           | 525       | 458       | 1.10                            | 2.32            | 52.0                  |
| 6           | 257       | 183       | 0.86                            | 0.694           | 92.6                  |
|             |           |           |                                 | Mean $\pm$ SD   | 88.1 $\pm$ 18.1       |

The pulse frequency, ratio-of-ratios, and cerebral arterial oxygen saturation were estimated from 60-s samples of the signals

**Table 2** Mean ( $\pm$ SD) cerebral arterial saturation and other variables estimated from long-duration measurement

| $f_{card}$ (Hz)     | Normalized peak amplitude/ $10^{-3}$ |                       | Oxygen saturation ScaO <sub>2</sub> (%) |
|---------------------|--------------------------------------|-----------------------|---|
|                     | $A_{card,IR}/A_{DC,IR}$              | $A_{card,R}/A_{DC,R}$ |   |
| 1.05 ( $\pm 0.12$ ) | 1.63 ( $\pm 0.73$ )                  | 1.29 ( $\pm 0.74$ )   | 90.54 ( $\pm 2.73$ )                    |

(<20 mmHg) for the majority of the monitoring period. There was a gradual decrease in ICP for the first 4 h, punctuated by a period of raised ICP ( $t = 110$ – $150$  min). There was also a gradual rise in ICP for the last 2 h of the monitoring period, although levels did not rise above normal for more than a few minutes toward the end of the monitoring period. This increase coincided with apparent spurious values observed in systemic mean arterial pressure (MAP) and ICP, seemingly caused by the patient beginning to regain consciousness and moving intermittently. The observed trend in ScaO<sub>2</sub> is similar to that seen in the ICP. No notable trends were observed in MAP or CPP, however, the MAP showed an increase, which coincided with the ICP rise ( $t = 110$ – $150$  min). There were also episodes after  $t = 220$  min where the patient was moving and the MAP rose above normal values. The EtCO<sub>2</sub> was seen to decrease gradually throughout the monitoring period, but remained within normal clinical ranges.

## Discussion

This pilot study was designed to provide a preliminary evaluation of a new monitoring technology. These preliminary results demonstrated that satisfactory quality red and near-infrared PPG signals can be obtained directly from human brain tissue using a fiber-optic probe and a cranial bolt as a conduit for the fibers. Further studies are needed to allow a more detailed analysis of the technique and to verify whether it offers advantages over existing monitoring technologies. It is hoped that the oxygen saturation measurements obtained with this system would be less susceptible to inaccuracy caused by extra-cerebral absorption, as has been shown to be the case with NIRS. Another potential advantage is lower sensitivity to hemorrhage around the probe tip, a phenomenon which causes uncertainty with PbrO<sub>2</sub> measurements. Since our system is based on pulse oximetry, whereby oxygen saturation is calculated from the ratio of two normalized optical signals, it was suggested that blood collecting around the fibers would not adversely affect the values. More studies are needed to prove this hypothesis since no appreciable loss of signal due to blood collecting around the probe was seen and visible inspection of the insertion sites revealed, in the worst case, only minor hemorrhage.

At present it is unclear why one of the patients (Patient No. 3) exhibited large ventilator artifact. One possible explanation is transfer of mechanical movement from the ventilator to the head or fibers. It is also possible that the patient had a lower than normal circulating volume. Hypovolemia, caused for example by blood loss, is known to cause periodic variations in blood pressure synchronous with mechanical ventilation [20].

**Fig. 5** The upper graph is a plot of ScaO<sub>2</sub> (brain), SpO<sub>2</sub> (finger), and SaO<sub>2</sub> (blood sample) plotted against time recorded during the long-duration measurement. The lower graph is a plot of intracranial pressure (ICP) against time

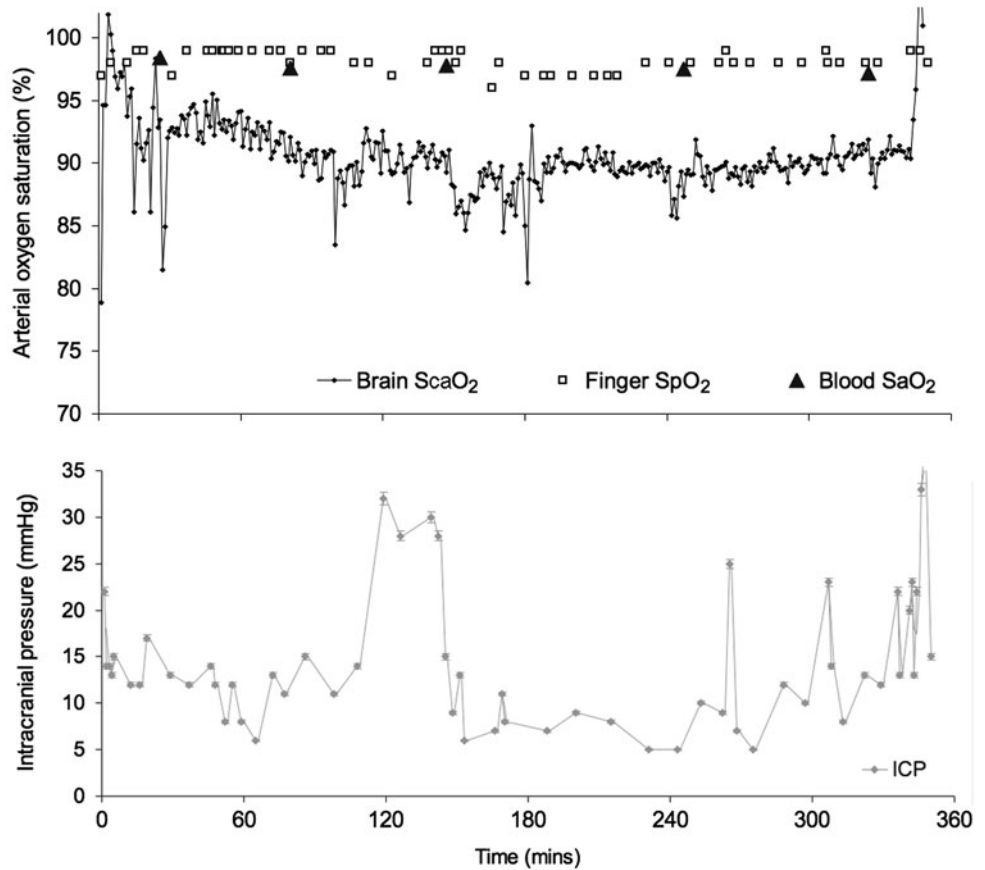
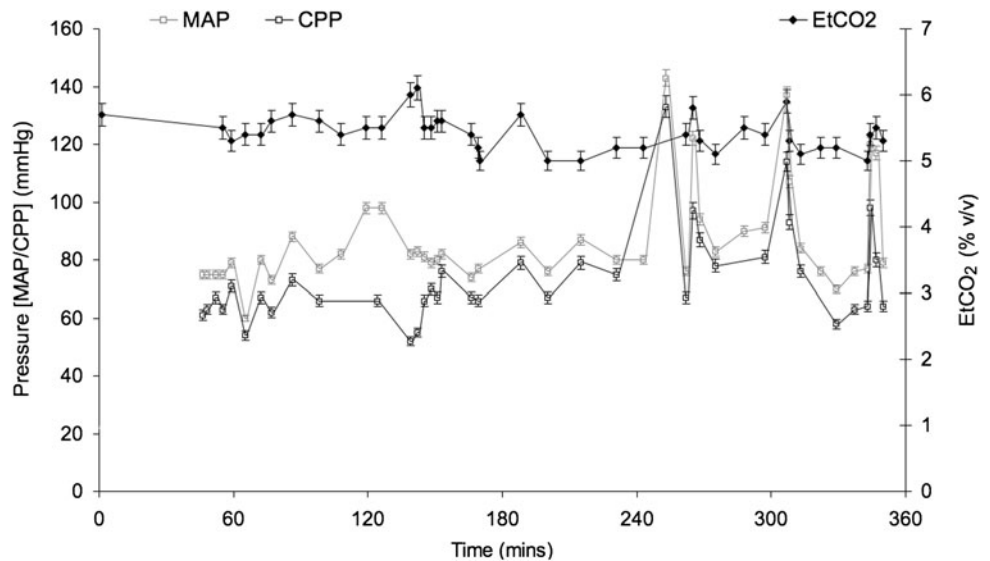


**Fig. 6** Graph showing mean arterial pressure (MAP), calculated cerebral perfusion pressure (CPP), and end-tidal CO<sub>2</sub> (EtCO<sub>2</sub>) plotted against time



The oxygen saturation values calculated for Patient No. 5 are considerably lower than the results obtained for the other patients. The finger pulse oximeter reading indicated a value of 99% for the systemic arterial oxygen saturation in this patient. This result could be explained if a high proportion of the blood in the pulsating vessels close to the probe contained blood of low oxygen saturation. This effect may be unusual, and may have arisen as a result of

the patient's individual pathology. Alternatively the cerebral veins may be pulsatile in all patients but the effect is not apparent unless the probe is positioned in a region where the density of veins is particularly high. The incompressibility of the brain cerebrospinal fluid and other cranial contents provides a likely mechanism for venous pulsation. Changes in cerebral arterial pressure during the cardiac cycle would cause the total volume of the cerebral



arteries to increase. The ICP would increase momentarily, compressing the cerebral veins so the veins are partially emptied of blood, causing their diameter to decrease. The proximity of a large vein to the probe tip seems a possible explanation for the extremely low cerebral arterial oxygen saturation reported for Patient No. 5. Unfortunately, the exact position of large cerebral blood vessels is not known prior to the burr hole being drilled and the placement of the bolt. Even after the burr hole is made, the situation does not really improve as the dura mater covers the cerebral surface and the large vessels running over it. If venous pulsation occurs in all cerebral tissue, it would complicate the process of estimating arterial oxygen saturation using the principle of pulse oximetry. The PPG signal, assumed to arise solely from pulsating arterial blood would be 'contaminated' by the venous pulse. Until more measurements are made, the extent of this potential problem is difficult to quantify.

For the long-duration measurement, it is not clear why the oxygen saturation measured in the frequency domain ( $ScaO_2$ ) was significantly lower than the finger  $SpO_2$  and the blood  $SaO_2$ : mean difference ( $ScaO_2 - SpO_2$ ) =  $-7.81(\pm 2.9)\%$ , ( $ScaO_2 - SaO_2$ ) =  $-7.37(\pm 2.8)\%$ . Although the arterial  $SpO_2$  and  $ScaO_2$  were measured at different sites, the brain and the finger, no significant difference in these values was expected. One possible explanation is that a component of the cardiac pulsation 'seen' by the probe in the brain was due to veins rather than arteries as was suggested to explain the extremely low oxygen saturation recorded in the short-duration measurements for Patient No. 5.

The results of this study are encouraging and warrant further evaluation of this technique to establish whether good quality signals can be maintained for a clinically relevant monitoring period in other patients, and to compare oxygen saturation values obtained using this method with those from other observations such as NIRS. These studies will hopefully indicate whether the technique may overcome the problems associated with NIRS and  $PbtO_2$  monitoring and become established as a useful monitoring modality in its own right.

## References

1. Hinds CJ, Watson JD. Intensive care: a concise textbook. 3rd ed. London: Saunders Ltd.; 2008.
2. Marik PE, Varon J, Trask T. Management of head trauma. *Chest*. 2002;122(2):699–711.

3. Graham DI, Adams JH, Doyle D, et al. Ischaemic brain damage is still common in fatal non-missile head injury. *J Neurol Neurosurg Psychiatry*. 1989;52:346–50.
4. Bartlett J, Kett-White R, Mendelow AD, Miller JD, Pickard J, Teasdale G. Guidelines for the initial management of head injuries: recommendations from the Society of British Neurological Surgeons. *Br J Neurosurg*. 1998;12:349–52.
5. Chesnut RM, Marshall LF, Klauber MR, et al. The role of secondary brain injury in determining outcome from severe head injury. *Journal of Trauma*. 1993;34:216–22.
6. Valadka AB, Gopinath SP, Contant CF, Uzura M, Robertson CS. Relationship of brain tissue  $PO_2$  to outcome after severe head injury. *Crit Care Med*. 1998;26(9):1576–81.
7. Schell RM, Cole DJ. Cerebral monitoring: jugular venous oximetry. *Anesth Analg*. 2000;90(3):559–66.
8. Kirkpatrick PJ. Use of near-infrared spectroscopy in the adult. *Philos Trans R Soc Lond B*. 1997;352(1354):701–5.
9. Ferrari M, Mottola L, Quaresima V. Principles, techniques, and limitations of near infrared spectroscopy. *Can J Appl Physiol*. 2004;29(4):463–87.
10. Hiraoka M, Firbank M, Essenpreis M, et al. A Monte Carlo investigation of optical pathlength in inhomogeneous tissue and its application to near-infrared spectroscopy. *Phys Med Biol*. 1993;38(12):1859–76.
11. Germon TJ, Kane NM, Manara AR, Nelson RJ. Near-infrared spectroscopy in adults: effects of extracranial ischaemia and intracranial hypoxia on estimation of cerebral oxygenation. *Br J Anaesth*. 1994;73(4):503–6.
12. Germon TJ, Young AE, Manara AR, Nelson RJ. Extracerebral absorption of near infrared light influences the detection of increased cerebral oxygenation monitored by near infrared spectroscopy. *J Neurol Neurosurg Psychiatry*. 1995;58(4):477–9.
13. van den Brink WA, Haitzma IK, Avezaat CJ, Houtsmuller AB, Kros JM, Maas AI. Brain parenchyma/ $pO_2$  catheter interface: a histopathological study in the rat. *J Neurotrauma*. 1998;15(10):813–24.
14. Phillips JP, Kyriacou PA, George KJ, Priestley JV, Langford RM. An optical fiber photoplethysmographic system for central nervous system tissue. In: Conference Proceedings of Annual International Conference of the IEEE Engineering in Medicine & Biology Society, vol. 1, p. 803–6, 2006.
15. Mortara RW. Intracranial pressure monitoring in the emergency setting. *Med Instrum*. 1982;16(4):197–8.
16. Ghajar J. Intracranial pressure monitoring techniques. *New Horizons*. 1995;3(3):395–9.
17. Barash PG, Cullen BF, Stoelting RK. Clinical anesthesia. 5th ed. Philadelphia: Lippincott Williams and Wilkins; 2006.
18. Phillips JP, Langford RM, Kyriacou PA, Jones DP. Preliminary evaluation of a new fibre-optic cerebral oximetry system. *Physiol Meas*. 2008;29(12):1383–96.
19. Moyle J. Pulse oximetry (principles and practice). 2nd ed. London: BMJ Books; 2002.
20. Szold A, Pizov R, Segal E, Perel A. The effect of tidal volume and intravascular volume state on systolic pressure variation in ventilated dogs. *Intensive Care Med*. 1989;15(6):368–71.